Chitosan-shelled oxygen-loaded nanodroplets abrogate hypoxia dysregulation of human keratinocyte gelatinases and inhibitors: New insights for chronic wound healing

Chitosan-shelled oxygen-loaded nanodroplets abrogate hypoxia dysregulation of human keratinocyte gelatinases and inhibitors: new insights for chronic wound healing.

Running head: Anti-hypoxia chitosan nanodroplet effects on keratinocyte MMPs and TIMPs.

Amina Khadjavi[1], Chiara Magnetto[2], Alice Panariti[3], Monica Argenziano[4], Giulia Rossana Gulino[5], Ilaria Rivolta[3], Roberta Cavalli[4], Giuliana Giribaldi[5], Caterina Guiot[#,1], Mauro Prato[#,1,6,*]

[1] *Dipartimento di Neuroscienze, Università di Torino, Torino, Italy*

[2] *Istituto Nazionale di Ricerca Metrologica (INRIM), Torino, Italy*

[3] *Dipartimento di Scienze della Salute, Università di Milano Bicocca, Monza, Italy*

[4] *Dipartimento di Scienza e Tecnologia del Farmaco, Università di Torino, Torino, Italy*

[5] *Dipartimento di Oncologia, Università di Torino, Torino, Italy*

[6] *Dipartimento di Scienze della Sanità Pubblica e Pediatriche, Università di Torino, Torino, Italy*

# equal contribution to the work

* Corresponding author: Dr. Mauro Prato, Dipartimento di Neuroscienze, Università di Torino, Corso Raffaello 30, 10125 Torino, Italy; Phone: +39-011-670-8198; Fax: +39-011-670-8174; E-mail: mauro.prato@unito.it

Funding sources: The work was funded by Compagnia di San Paolo (Ateneo-San Paolo 2011 ORTO11CE8R grant to CG and MP) and Università di Torino (ex-60% 2013 intramural funds to GG and MP).

Conflict of interest disclosure: The authors have no conflicting financial interests.

Text word count: 3391. *No. references*: 30. *No. figures*: 7. *No. tables*: 2.

Abstract

BACKGROUND: In chronic wounds, efficient epithelial tissue repair is hampered by hypoxia, and balances between the molecules involved in matrix turn-over such as matrix metalloproteinases (MMPs) and tissue inhibitors of metalloproteinases (TIMPs) are seriously impaired. Intriguingly, new oxygenating nanocarriers such as 2H,3H-decafluoropentane-based oxygen-loaded nanodroplets (OLNs) might effectively target chronic wounds.

OBJECTIVE: To investigate hypoxia and chitosan-shelled OLN effects on MMP/TIMP production by human keratinocytes.

METHODS: HaCaT cells were treated for 24 h with 10% v/v OLNs both in normoxia or hypoxia. Cytotoxicity and cell viability were measured through biochemical assays; cellular uptake by confocal microscopy; MMP and TIMP production by enzyme-linked immunosorbent assay or gelatin zymography.

RESULTS: Normoxic HaCaT cells constitutively released MMP-2, MMP-9, TIMP-1 and TIMP-2. Hypoxia strongly impaired MMP/TIMP balances by reducing MMP-2, MMP-9, and TIMP-2, without affecting TIMP-1 release. After cellular uptake by keratinocytes, nontoxic OLNs abrogated all hypoxia effects on MMP/TIMP secretion, restoring physiological balances. OLN abilities were specifically dependent on time-sustained oxygen diffusion from OLN core.

CONCLUSION: Chitosan-shelled OLNs effectively counteract hypoxia-dependent dysregulation of MMP/TIMP balances in human keratinocytes. Therefore, topical administration of exogenous oxygen, properly encapsulated in nanodroplet

formulations, might be a promising adjuvant approach to promote healing processes in hypoxic wounds.

Keywords: chitosan; nanodroplet; hypoxia; matrix metalloproteinase (MMP); tissue inhibitor of metalloproteinase (TIMP); keratinocyte.

Highlights

- Hypoxia impairs MMP9/TIMP1 and MMP2/TIMP2 balances in HaCaT human keratinocytes.
- Chitosan-shelled oxygen-loaded nanodroplets (OLNs) are internalised by HaCaT cells.
- OLNs are not toxic to HaCaT cells.
- OLNs effectively counteract hypoxia effects on MMP/TIMP balances in HaCaT cells.
- OLNs appear as promising and cost-effective therapeutic tools for hypoxic wounds.

Introduction

The epidermis is a stratified squamous epithelium consisting of several cell types, including Langerhans cells, melanocytes, and keratinocytes, that provide a physical barrier to protect the organism from external agents and pathogens, and to limit fluid loss.[1] Highly specialised keratinocytes, by far the most abundant epidermal cell type, not only maintain the epidermis but also restore its integrity after injury.[2] Wound healing is a complex multi-step process comprised of three continuous and overlapping phases (inflammation, re-epithelialisation, and remodelling) requiring highly orchestrated temporal and spatial regulation of various cell types and mediators in the damaged tissue area.[2] As the barrier is disrupted upon acute skin injury, neutrophils, monocytes, and macrophages are recruited to the site of injury.[3] Subsequently, keratinocytes undergo activation through changes in the cytoskeleton network and expression of cell surface receptors essential for re-epithelialisation, allowing keratinocytes to migrate into the wound.[2]

For the wound to heal successfully, keratinocytes should be able not only to detach from the underlying basal lamina but also to move and migrate through the newly synthesised extracellular matrix (ECM) of the wound, a process facilitated by matrix metalloproteinases (MMPs).[4] These evolutionarily conserved and tightly regulated zinc-dependent proteases are produced by a broad spectrum of specialised cells, including keratinocytes, fibroblasts, endothelial cells, and immune cells, and serve essential roles in cell survival, proliferation, migration, invasion, haemostasis and inflammation.[5] Some MMPs typically involved in wound healing are MMP-1, -2, -3, -9, -10, -14, -19, and -28.[2,4] Importantly, optimal keratinocyte migration during wound closure depends

on tight regulation of balances between MMPs and tissue inhibitors of metalloproteinases (TIMPs), whereas dysregulated MMP/TIMP ratios demarcate chronic nonhealing wounds.[6]

Among the prominent microenvironmental factors associated with tissue injury and repair, hypoxic responses have been shown to be critically involved in virtually all processes of wound healing and remodelling.[7-8] However, molecular and cellular mechanisms underlying hypoxic regulation of wound healing are still poorly understood. When a pro-inflammatory milieu associated with hypoxia, increased proteases, and bacterial burden develops around the wound, it fails some or all the stages which lead to healing, thus becoming chronic.[9] Diabetes-associated vasculopathies and pressure ulcers are typical examples of chronic wounds sharing hypoxia as a main clinical feature.[10]

To counteract hypoxia, several systems for oxygen release, including haemoglobin- and perfluorocarbon-based oxygen carriers, have been developed in the last years.[11] The known benefits of nanotechnology, including size, stability, and controlled drug release,[12] combined with the emerging advantages of ultrasound (US)-triggered transdermal drug delivery[13] have paved the way to develop nonconventional and innovative therapies for infected chronic wounds. In particular, US-responsive perfluoropentane-cored oxygen-loaded nanobubbles and decafluoropentane (DFP)-cored oxygen-loaded nanodroplets (OLNs), both coated with biocompatible and biodegradable polysaccharides such as chitosan or dextran, recently proved effective in releasing oxygen either *in vitro* or *in vivo*.[14-17]

In this work, the effects of hypoxia on the production of gelatinases (MMP-2 and -9) and their inhibitors (TIMP-1 and -2) by human HaCaT keratinocytes were investigated.

Next, the potential abilities of new chitosan-shelled OLNs to counteract these effects were thoroughly evaluated.

Materials and Methods

Materials

All materials were from Sigma-Aldrich, St Louis, MO, unless otherwise stated. Sterile plastics were from Costar, Cambridge, UK; Panserin 601 medium was from PAN Biotech, Aidenbach, Germany; ELISA kit for hMMP-2 was from Abnova, Taipei City, Taiwan; ELISA kits for hMMP-9, hTIMP-1 and hTIMP-2 were from RayBiotech, Norcross, GA; electrophoresis reagents and computerised densitometer Geldoc were from Bio-rad Laboratories, Hercules, CA; Synergy HT microplate reader was from Bio-Tek Instruments, Winooski, VT; ethanol (96%) was from Carlo Erba (Milan, Italy); Epikuron 200® (soya phosphatidylcholine 95%) was from Degussa (Hamburg, Germany); palmitic acid, decafluoropentane (DFP), chitosan (medium MW), and polyvinylpyrrolidone (PVP) were from Fluka (Buchs, Switzerland); ultrapure water was obtained using a 1-800 Millipore system (Molsheim, France); Ultra-Turrax SG215 homogeniser was from IKA (Staufen, Germany); Delsa Nano C analyser was from Beckman Coulter (Brea, CA); LDO oxymeter was from Hach Lange (Salford, UK); Philips CM10 instrument was from Philips (Eindoven, The Netherlands); XDS-3FL microscope was from Optika (Ponteranica, Italy). Recombinant human MMP-9 was generously gifted by Prof. Ghislain Opdenakker and Prof. Philippe Van den Steen, Laboratory of Immunobiology, Catholic University of Leuven, Belgium.

Cell cultures

HaCaT, a long-term cell line of human keratinocytes immortalised from a 62-year old Caucasian male donor,[18] was used for assessment of OLN biocompatibility. Cells were

grown as adherent monolayers in Dulbecco's modified Eagle's medium (DMEM) supplemented with 10% foetal bovine serum (FBS), 100 U/ml penicillin, 100 μg/ml streptomycin (PEN-STREP) and 2 mM L-glutamine in a humidified CO_2/air-incubator at 37°C. Before starting the experiments, cells were washed with PBS, detached with trypsin/ethylenediaminetetraacetic acid (EDTA) (0.05/0.02 % v/v), washed with fresh medium and plated at a standard density (10^6 cells/well in 6-well plates) in 2 ml serum-free Panserin 601 medium.

Chitosan nanodroplet preparation and characterisation

OLNs, oxygen-free nanodroplets (OFNs), and oxygen-saturated solution (OSS) were prepared as previously described.[16] Briefly, 1.5 ml DFP, 0.5 ml polyvinylpyrrolidone and 1,8 ml Epikuron® 200 (solved in 1% w/v ethanol and 0.3 % w/v palmitic acid solution) were homogenised in 30 ml phosphate-buffered saline (PBS) solution (pH 7.4) for 2 min at 24000 rpm by using Ultra-Turrax SG215 homogeniser. For OLNs, the solution was saturated with O_2 for 2 min. Finally, 1.5 ml chitosan or fluorescein isothiocyanate (FITC)-labelled chitosan solution was added drop-wise whilst the mixture was homogenised at 13000 rpm for 2 min. For OFN and OSS PBS formulations, OLN preparation protocol was applied omitting O_2 or chitosan/DFP addition, respectively. Immediately after manufacturing, nanodroplets were sterilised through ultraviolet (UV)-C ray exposure for 20 min and characterised for: morphology, by transmission electron microscopy (TEM); size distribution, polydispersity index, and zeta potential, by dynamic light scattering; and oxygen content through a chemical assay as previously described[16]. OLNs, OFNs and OSS were also challenged for their oxygen delivery abilities by monitoring oxygen release into Panserin 601 cell culturing

medium up to 24 h through Hach Langhe LDO oxymeter, displaying an accuracy of 0.01 mg/l. The oxymeter was calibrated in air, waiting for stable temperature and humidity conditions to be reached before each measurement.

OLN cytotoxicity studies

The potential cytotoxic effects of OLN and control formulations were measured as the release of lactate dehydrogenase (LDH) from HaCaT cells into the extracellular medium as previously described.[19] Briefly, cells were incubated in Panserin 601 medium for 24 h in the presence or absence of increasing doses (5%, 10%, and 20% v/v) of OLNs or 10% v/v OFNs or OSS, either in normoxic (20 % O_2) or hypoxic (1 % O_2) conditions, in a humidified CO_2/air-incubator at 37°C. Then, 1 ml of cell supernatants was collected and centrifuged at 13000*g* for 2 min. Cells were washed with fresh medium, detached with trypsin/ EDTA (0.05/0.02 % v/v), washed with PBS, resuspended in 1 ml of TRAP (82.3 mM triethanolamine, pH 7.6), and sonicated on ice with a 10 s burst. 5 µl of cell lysates and 50 µl of cell supernatants were diluted with TRAP and supplemented with 0.5 mM sodium pyruvate and 0.25 mM NADH (300 µL as a final volume) to start the reaction. The reaction was followed measuring the absorbance at 340 nm (37 °C) with Synergy HT microplate reader. Both intracellular and extracellular enzyme activities were expressed as µmol of oxidised NADH/min/well. Finally, cytotoxicity was calculated as the net ratio between extracellular and total (intracellular + extracellular) LDH activities.

Cell viability studies

Cell viability was evaluated using 3-(4,5-dimethylthiazol-2-yl)-2,5-diphenyltetrazolium bromide (MTT) assay. HaCaT cells were incubated in Panserin 601 medium for 24 h with/without increasing doses (5%, 10%, and 20% v/v) of OLNs or 10% v/v OFNs or OSS, either in normoxic (20 % O_2) or hypoxic (1 % O_2) conditions, in a humidified CO_2/air-incubator at 37°C. Thereafter, 20 µL of 5 mg/mL MTT in PBS were added to cells for 3 additional hours at 37 °C. The plates were then centrifuged, the supernatants discarded and the dark blue formazan crystals dissolved using 100 µL of lysis buffer containing 20 % (w/v) sodium dodecyl sulfate (SDS), 40 % N,N-dimethylformamide (pH 4.7 in 80 % acetic acid). The plates were then read on Synergy HT microplate reader at a test wavelength of 550 nm and at a reference wavelength of 650 nm.

Evaluation of OLN uptake by human keratinocytes

HaCaT cells were plated in 24-well plates on glass coverslips and incubated in Panserin 601 medium for 24 h with/without 10% v/v FITC-labelled OLNs in a humidified CO_2/air-incubator at 37°C. After 4',6-diamidino-2-phenylindole (DAPI) staining to visualise cells nuclei, fluorescence images were acquired by a LSM710 inverted confocal laser scanning microscope equipped with a Plan-Neofluar 63×1.4 oil objective, that allowed a field view of at least 5 cells. Wavelength of 488 nm was used to detect OLNs, and of 460 nm to detect the labelled nuclei. The acquisition time was 400 ms.

Measurement of latent and active forms of gelatinases in cell supernatants

The levels of latent and active forms of MMP-2 and MMP-9 were evaluated by gelatin zymography in cell supernatants as previously described.[20] Briefly, HaCaT cells were incubated in serum-free Panserin 601 medium for 24 h with/without 10% v/v OLNs,

OFNs or OSS, either in normoxic (20 % O_2) or hypoxic (1 % O_2) conditions, in a humidified CO_2/air-incubator at 37°C. Thereafter, 15 µl cell supernatants/lane were loaded on 8% polyacrylamide gels containing 0.1% gelatin under nondenaturing and nonreducing conditions. Following electrophoresis, gels were washed at room temperature for 2 h in milliQ water containing 2.5% (v/v) Triton-X100 and incubated for 18 h at 37°C in a collagenase buffer containing (mM): NaCl, 200; Tris, 50; $CaCl_2$, 10; and 0.018% (v/v) Brij 35, pH 7.5, with or without 5 mM EDTA to exclude aspecific bands. At the end of the incubation, the gels were stained for 15 min with Coomassie blue (0.5% Coomassie blue in methanol/acetic acid/water at a ratio of 30:10:60). The gels were destained in milliQ water. Densitometric analysis of the bands, reflecting the total levels of latent and active forms of MMP-2 and MMP-9, was performed using a computerised densitometer.

Measurement of MMP-2, MMP-9, TIMP-1, and TIMP-2 production

HaCaT cells were incubated in Panserin 601 medium for 24 h with/without 10% v/v OLNs, OFNs or OSS, either in normoxic (20 % O_2) or hypoxic (1 % O_2) conditions, in a humidified CO_2/air-incubator at 37°C. Thereafter, cell supernatants were collected, and the levels of MMP-2, MMP-9, TIMP-1, and TIMP-2 were assayed in 100 µl of cell supernatants by specific ELISA. Standard calibration curves were generated with rhMMP-2, rhMMP-9, rhTIMP-1, and rhTIMP-2, according to the manufacturer's instructions.

Statistical analysis.

For each set of experiments, data are shown as means+SEM or as representative images from three independent experiments with similar results. All data were analysed by a one-way Analysis of Variance (ANOVA) followed by Tukey's post-hoc test (software: SPSS 16.0 for Windows, SPSS Inc., Chicago, IL).

Results

Physico-chemical characterisation and oxygen release abilities of chitosan nanodroplet preparations

Before being employed in the biological studies, all OLN and OFN preparations were meticulously characterized for morphology, size distribution, polydispersity index, zeta potential, and oxygen content. Furthermore, OLN ability to release oxygen into Panserin 601 cell culturing medium was monitored up to 24 h in comparison with OFNs and OSS. As shown in **Figure 1** and **Tables 1-2**, the obtained results were always in line with literature data[16]. Both OLNs and OFNs displayed spherical shapes. All sizes were in the nanometer range, with average diameters ranging from ~250 nm (OFNs) to ~750 nm (OLNs). Average polidispersity indexes were 0.23 and 0.12 for OLN and OFN preparations, respectively. Zeta potentials ranged from ~ + 34 mV (OFNs) to ~ + 35 mV (OLNs). OLNs also displayed a good oxygen-storing capacity (~ 0.45 mg/ml of oxygen, not shown). Furthermore, OLN and OFN preparations resulted physically stable over time, as confirmed by long-term checking of these parameters (up to six months). Finally, OLN preparations proved effective in releasing high and clinically relevant oxygen amounts (~10-16 mg/L) into Panserin 601 cell culturing medium up to 24 h. On the contrary, the oxygen levels released by OSS appeared to be high (~13 mg/L) only at the earlier time-points of the observational period (0-2 h), rapidly decreasing and eventually becoming negligible for the rest of the observational period. As expected, oxygen release from OFN preparations was always negligible.

Chitosan OLN effects on human keratinocyte viability

Chitosan OLN toxicity was evaluated by testing *in vitro* cultures of human HaCaT keratinocytes. As shown in **Figure 2** (Panel a: LDH assay; Panel b: MTT assay), increasing volumes of chitosan OLN PBS suspensions (100, 200, and 400 μl) were not toxic to HaCaT keratinocytes (10^6 cells/2 ml Panserin 601 cell culture medium) after 24 h-incubation both in normoxic (20% O_2) and hypoxic (1% O_2) conditions. Therefore, the intermediate chitosan OLN dosage was chosen to perform the subsequent experiments. Toxicity of chitosan OFNs and OSS (controls) was also assayed (Panel 1C: LDH assay; Panel 1D: MTT assay). OSS did not show cytotoxicity, whereas OFNs slightly reduced the viability of treated cells with respect to untreated cells.

Chitosan OLN internalisation by human keratinocytes

To check whether chitosan OLNs were uptaken by human keratinocytes, a confocal microscopy approach was chosen. HaCaT keratinocytes (10^6 cells/2 ml cell culture medium) were incubated with or without 200 μl FITC-labelled chitosan OLN PBS suspensions for 24 h in normoxic conditions. As shown in **Figure 3**, OLNs were avidly internalised by human keratinocytes.

Hypoxia and chitosan OLN effects on gelatinase secretion by human keratinocytes

After 24 h-incubation of HaCaT keratinocytes (10^6 cells/2 ml cell culture medium) with or without 200 chitosan OLNs, chitosan OFN or OSS, both in normoxic (20% O_2) and hypoxic (1% O_2) conditions, the secretion of MMP-2 and MMP-9 protein forms was evaluated by gelatin zymography and subsequent densitometry. As shown in **Figure 4**, normoxic untreated HaCaT cells constitutively released either the latent or the activated forms of MMP-2. ProMMP-9 protein was also found in cell supernatants, however

active MMP-9 was absent. Hypoxia significantly reduced the levels of all these molecules. In the presence of OLNs the levels of proMMP-2, MMP-2, and proMMP-9 in hypoxic conditions were similar to those detected in normoxic conditions, demonstrating that OLNs effectively abrogated all hypoxia effects on gelatinase secretion. Interestingly, hypoxia-counteracting action of OLNs was not mimicked by OFNs or OSS. Thereafter, these results were quantitatively confirmed by complementary ELISA (see **Figure 5**). As an average, normoxic untreated HaCaT cells constitutively secreted ~1600 pg/ml MMP-2 and ~430 ng/ml MMP-9. Hypoxia significantly reduced MMP-2 and MMP-9 secretion by 50% and 20%, respectively. Again, OLNs - but not OFNs and OSS - fully abrogated hypoxia effects, restoring normoxic MMP-2 and MMP-9 levels.

Hypoxia and chitosan OLN effects on balances between gelatinases and their inhibitors secreted by human keratinocytes

HaCaT keratinocytes (10^6 cells/2 ml cell culture medium) were incubated for 24 h with or without 200 chitosan OLNs, chitosan OFN or OSS, both in normoxic (20% O_2) and hypoxic (1% O_2) conditions. Thereafter, the secretion of TIMP-1 and TIMP-2 was evaluated by ELISA. As shown in **Figure 6**, normoxic untreated HaCaT cells constitutively released ~16 ng/ml TIMP-1 and ~600 pg/ml TIMP-2. Hypoxia did not affect TIMP-1 production while it significantly reduced by almost 20% the secreted levels of TIMP-2. OLNs fully abrogated hypoxia effects, restoring physiological TIMP-2 amounts also in hypoxic culturing conditions. OFNs and OSS did not reproduce OLN effects. As a next step, the balances between gelatinases and their inhibitors were calculated as MMP-9/TIMP-1 and MMP-2/TIMP-2 stoichiometric ratios. As shown in

Figure 7, hypoxia significantly reduced either ratio by ~25%. OLNs effectively counteracted hypoxia effects, restoring the physiological MMP/TIMP balances.

Discussion

The present study investigated the effects of hypoxia, along with the therapeutic potential of chitosan-shelled and DFP-cored OLNs, on the secretion of gelatinases (MMP-2 and MMP-9) and their physiological inhibitors (TIMP-2 and TIMP-1, respectively) by human keratinocytes.

Based on the available literature data, hypoxia effects on keratinocyte MMPs are highly variable depending on the donor's age.[21] Since hypoxia-associated skin pathologies such as chronic wounds are generally more frequent in the elderly, in the present study a keratinocyte cell line immortalised from a 62-year old donor (HaCaT) was employed.[18] Normoxic keratinocytes constitutively released MMP-2 (both latent and active forms) and MMP-9 (latent form), as well as TIMP-1 and TIMP-2, in line with previous reports on HaCaT cells.[22] Notably, hypoxia strongly impaired the balances between gelatinases and their inhibitors by reducing MMP-2, MMP-9, and TIMP-2, without affecting TIMP-1 secretion. To the best of our knowledge, this is the first evidence on hypoxia-dependent dysregulation of gelatinases and their inhibitors that is available from HaCaT cells. Intriguingly, these results are consistent with those obtained by Xia and colleagues on primary cultures of human keratinocytes isolated from ≥60-year old donors.[21]

Once determined the entity of hypoxia-dependent dysregulation of MMP/TIMP balances, OLNs were challenged as potential tools to counteract hypoxia effects. Chitosan-shelled and DFP-cored OLNs, characterised by spherical shape, 700 nm average diameters, and cationic surfaces,[16] were chosen as candidate therapeutic tools for several reasons. First, cationic nanoparticles are generally recommended for topical

treatment due to the anionic nature of the skin.[23] Second, OLNs have recently proven effective in delivering oxygen to both *in vitro* and *in vivo* models of hypoxic skin.[16] Finally, OLNs have displayed cytostatic activity against methicillin-resistant *Staphylococcus aureus* and *Candida albicans*, as a likely consequence of the presence of antimicrobial chitosan in their shell.[24] As such, OLNs have been proposed as promising candidates to treat hypoxic and infected chronic wounds.

Notably, all OLNs employed in the present work displayed spherical shapes, sizes in the nanometer range (~750 nm), positive zeta potentials (~ + 35 mV), good oxygen-storing capacity (~ 0.45 mg/ml of oxygen), and long-term stability, in line with literature data[16]. Furthermore, OLN preparations proved effective in releasing high and clinically relevant oxygen amounts into Panserin 601 cell culturing medium up to 24 h, opposite to OSS (able to increase oxygen levels only for a few hours) and OFNs (not releasing significant oxygen amounts).

OLN biocompatibility was firstly assessed by treating HaCaT cells with different concentrations (5-20% v/v) of nanodroplet PBS formulations. Interestingly, OLNs were avidly uptaken by human keratinocytes. Note that in human keratinocytes the lateral dimensions range between 35 and 55 μm while typical height is10 ± 3 μm.[25] Besides, keratinocytes have been reported to expose several anionic sites on their plasma membrane.[26] These characteristics are fully compatible with OLN nanometric dimensions and positive surface charge, thus justifying OLN adhesion on keratinocyte membranes and following cellular internalisation, as observed here. Furthermore, OLNs did not display cytotoxic effects on human keratinocytes at any doses, either in normoxia or hypoxia. Therefore, the intermediate concentration (10% v/v) was chosen for the subsequent experiments. Interestingly, the presence of oxygen in the inner core

of OLNs seems to play a crucial role in avoiding cell toxicity. On the contrary, OFNs (but not OSS) slightly reduced keratinocyte viability. This might depend on the employed chitosan type (medium MW), as it has been reported that chitosan molecules exhibit a MW-dependent negative effect on HaCaT cell viability and proliferation *in vitro*.[27] On the other hand, as emerged from intensive research on toxicity and absorption, distribution, and excretion of neat and emulsified fluorocarbons, DFP is known to be extremely stable, biologically inert, and rapidly excreted into the expired air in a nonmetabolised form after injection into the bloodstream.[28]

OLNs fully abrogated hypoxia effects. Even in hypoxic culturing conditions, OLN-treated keratinocytes secreted normoxia-like levels of MMP-2, MMP-9, TIMP-1, and TIMP-2, and the physiological balances between gelatinases and their inhibitors were restored. Apparently, these effects were specifically dependent on time-sustained oxygen release from the inner core of OLNs, since they were neither reproduced by OFN nor OSS treatments. Intriguingly, these results are in full agreement with those obtained from parallel works investigating OLN abilities to restore normoxia-like MMP/TIMP balances in hypoxic human monocytes[29] and microvascular dermal endothelium[30], two cell populations playing relevant roles during wound healing processes[2-3].Taken altogether, these data indicate that hypoxia seriously hampers MMP/TIMP balances secreted by human keratinocytes, whereas chitosan-shelled and DFP-cored OLNs are effective in counteracting hypoxia effects, hopefully supporting optimal keratinocyte migration during wound closure. These results, combined with the intrinsic benefits of nanodroplets, including size, charge, stability, antimicrobial properties, controlled release, and suitability for further drug functionalisation, drug loading or encapsulation,[16-17, 24] strengthen the proposal that OLNs may potentially

serve as medical devices for preventive or adjuvant treatment of chronic wounds. Therefore, future preclinical and clinical studies to translate this technology to clinical practice are heavily encouraged.

Acknowledgements

The work was funded by Compagnia di San Paolo (Ateneo-San Paolo 2011 ORTO11CE8R grant to CG and MP) and Università di Torino (ex-60% 2013 intramural funds to GG and MP). MP holds a professorship granted by Università degli Studi di Torino and Azienda Sanitaria Locale-19 (ASL-19). The funders had no role in study design, data collection, data analysis, manuscript preparation and/or publication decisions. Thanks are due to Adriano Troia for suggestions on nanodroplet manufacturing, to Marco Soster for help with TEM analyses, to Francesca Silvagno for providing HaCaT cell line, and to Ghislain Opdenakker and Philippe Van den Steen for kindly gifting recombinant human MMP-9.

Conflict of interest disclosure

The authors have no conflicting financial interests.

References

1 Roberts N, Horsley V. Developing stratified epithelia: lessons from the epidermis and thymus. Wiley Interdiscip Rev Dev Biol 2014;3:389-402.

2 Pastar I, Stojadinovic O, Yin NC, et al. Epithelialization in wound healing: a comprehensive review. Adv Wound Care (New Rochelle) 2014;3:445-64.

3 Strbo N, Yin N, Stojadinovic O. Innate and adaptive immune responses in wound epithelialization. Adv Wound Care (New Rochelle) 2014;3:492-501.

4 Gill SE, Parks WC. Metalloproteinases and their inhibitors: regulators of wound healing. Int J Biochem Cell Biol 2008;40:1334-47.

5 Nagase H, Visse R, Murphy G. Structure and function of matrix metalloproteinases and TIMPs. Cardiovasc Res 2006;69:562-73.

6 Muller M, Trocme C, Lardy B, et al. Matrix metalloproteinases and diabetic foot ulcers: the ratio of MMP-1 to TIMP-1 is a predictor of wound healing. Diabet Med 2008;25:419-26.

7 Hong WX, Hu MS, Esquivel M, et al. The role of hypoxia-inducible factor in wound healing. Adv Wound Care (New Rochelle) 2014;3:390-9.

8 Ruthenborg RJ, Ban JJ, Wazir A, et al. Regulation of wound healing and fibrosis by hypoxia and hypoxia-inducible factor-1. Mol Cells 2014;37:637-43.

9 Montfrans CV, Stok M, Geerkens M. Biology of chronic wounds and new treatment strategies. Phlebology 2014;29:165-7.

10 Baltzis D, Eleftheriadou I, Veves A. Pathogenesis and treatment of impaired wound healing in diabetes mellitus: new insights. Adv Ther 2014;31:817-36.

11 Cabrales P, Intaglietta M. Blood substitutes: evolution from noncarrying to oxygen- and gas-carrying fluids. ASAIO J 2013;59:337-54.

12 Schroeter A, Engelbrecht T, Neubert RHH, Goebel ASB. New Nanosized Technologies for Dermal and Transdermal Drug Delivery. A Review. J Biomed Nanotechnol 2010;6:511–28.

13 Park D, Park H, Seo J, Lee S. Sonophoresis in transdermal drug deliverys. Ultrasonics 2014;54:56-65.

14 Cavalli R, Bisazza A, Rolfo A, et al. Ultrasound-mediated oxygen delivery from chitosan nanobubbles. Int J Pharm 2009;378:215-7.

15 Cavalli R, Bisazza A, Giustetto P, et al. Preparation and characterization of dextran nanobubbles for oxygen delivery. Int J Pharm 2009;381:160-5.

16 Magnetto C, Prato M, Khadjavi A, et al. Ultrasound-activated decafluoropentane-cored and chitosan-shelled nanodroplets for oxygen delivery to hypoxic cutaneous tissues. RSC Adv 2014;4:38433-41.

17 Prato M, Magnetto C, Jose J, et al. 2H,3H-decafluoropentane-based nanodroplets: new perspectives for oxygen delivery to hypoxic cutaneous tissues. Plos One 2015; 10:e0119769..

18 Boukamp P, Dzarlieva-Petrusevska RT, Breitkreuz D, et al. Normal keratinization in a spontaneously immortalized aneuploid human keratinocyte cell line. J Cell Biol 1988;106:761-71.

19 Polimeni M, Valente E, Ulliers D, et al. Natural haemozoin induces expression and release of human monocyte tissue inhibitor of metalloproteinase-1. PLoS One 2013;8:e71468.

20 Khadjavi A, Valente E, Giribaldi G, Prato M. Involvement of p38 MAPK in natural haemozoin- and 15-HETE-dependent MMP-9 enhancement in human adherent monocytes. Cell Biochem Funct 2014;32:5-15.

21 Xia YP, Zhao Y, Tyrone JW, et al. Differential activation of migration by hypoxia in keratinocytes isolated from donors of increasing age: implication for chronic wounds in the elderly. J Invest Dermatol 2001;116:50-6.

22 Yang H, Dai Y, Dong H, et al. Trichloroethanol up-regulates matrix metalloproteinase-9 and tissue inhibitor of metalloproteinase-1 in HaCaT cells. Toxicol in vitro 2011;25:1638-43.

23 Wu X, Landfester K, Musyanovych A, Guy RH. Disposition of charged nanoparticles after their topical application to the skin. Skin Pharmacol Physiol 2010;23:117-23.

24 Banche G, Prato M, Magnetto C, et al. Antimicrobial properties of chitosan-shelled oxygen-loaded nanodroplets: new insights for ultrasound-mediated adjuvant treatment of skin infection. Future Microbiol 2015; in press.

25. Lulevich V, Yang HY, Isseroff RR, Liu GY. Single cell mechanics of keratinocyte cells. Ultramicroscopy. 2010;110:1435-42

26. Schuler G, Polin G, Fritsch PO. Differences of cell surface label distribution and redistributionpatterns between mammalian keratinocytes and melanocytes in culture. J Invest Dermatol. 1981;77:347-52

27 Wiegand C, Winter D, Hipler UC. Molecular-weight-dependent toxic effects of chitosans on the human keratinocyte cell line HaCaT. Skin Pharmacol Physiol 2010;23:164-70.

28 Schutt EG, Klein DH, Mattrey RM, Riess JG. Injectable microbubbles as contrast agents for diagnostic ultrasound imaging: the key role of perfluorochemicals. Angew Chem Int Ed Engl 2003;42:3218-35.

29. Gulino GR, Magnetto C, Khadjavi A, et al. Oxygen-loaded nanodroplets effectively abrogate hypoxia dysregulating effects on secretion of matrix metalloproteinase-9 and tissue inhibitor of metalloproteinase-1 by human monocytes. Mediators Inflamm, 2015; 2015:964838.

30. Basilico N, Magnetto C, D'Alessandro S, et al. Oxygen nanodroplets restore angiogenic phenotype of hypoxic dermal endothelium. Wound Repair Regen, submitted.

Tables

TABLE 1. Diameters, polydispersity indexes and zeta potentials of OLN preparations employed in the biological studies

OLN preparation	diameter nm ± SD	polydispersity index	zeta potential mV ± SD
preparation no.1	710.40 ± 116.3	0.23	+35.56±1.00
preparation no.2	766.70 ± 142.4	0.22	+35.84±1.00
preparation no.3	735.57± 123.4	0.23	+34.97±1.00

TABLE 2. Diameters, polydispersity indexes and zeta potentials of OFN preparations employed in the biological studies

OFN preparation	diameter nm ± SD	polydispersity index	zeta potential mV ± SD
preparation no.1	222.8 ± 103.4	0.12	+34.74 ± 1.00
preparation no.2	263.7 ± 175.3	0.12	+34.69 ± 1.00
preparation no.3	245.1 ± 146.7	0.12	+34.57 ± 1.00

Figure Legends

FIGURE 1. Physico-chemical characterization and oxygen release abilities of chitosan nanodroplet preparations. After manufacturing, all nanodroplet preparations were meticulously characterized for morphology by TEM, for size distribution by dynamic light scattering, and for long-term ability to release oxygen into Panserin 601 cell culturing medium by oxymetry. Results are shown as representative images obtained from three different preparations. Panel (a). TEM image of OLNs. Magnification: 52000X. Panel (b). TEM image of OLNs. Magnification: 21000X. Panel (c). OLN size distribution. Panel (d). OFN size distribution. Panel (e). 24 h-monitoring of oxygen release from OLN, OFN, and OSS preparations into Panserin 601 cell culturing medium.

FIGURE 2. Hypoxia and chitosan OLN effects on human keratinocyte viability. HaCaT keratinocytes (10^6 cells/2 ml Panserin 601 medium) were left untreated or treated with increasing volumes (100-400 μl) of chitosan OLNs or with 200 μl chitosan OFNs, or OSS for 24 h in normoxia (20% O_2, black columns/squared-lines) or hypoxia (1% O_2, white columns/squared-lines). After collection of cell supernatants and lysates, cytotoxicity percentage was measured through LDH assay (panels a and c), whereas cell viability percentage was measured through MTT assay (panels b and d). Results are shown as means+SEM from three independent experiments. Data were also evaluated for significance by ANOVA: * vs normoxic control cells: *p* not significant (panels a-b), $p<0.0001$ (panel c), and $p<0.001$ (panel d); ° vs hypoxic control cells: *p* not significant (panels a-b), $p<0.0001$ (panel c), and $p<0.0001$ (panel d).

FIGURE 3. Chitosan OLN internalisation by HaCaT cell line. Human keratinocytes (10^6 cells/2 ml Panserin 601 medium) were left untreated (panels a-c) or treated with 200 μl FITC-labelled chitosan OLNs (panels d-f) for 24 h in normoxia (20 % O_2). After DAPI staining, cells were checked by confocal microscopy. Results are shown as representative images from three independent experiments. Panels (a) and (d): cell nuclei after DAPI staining (blue). Panels (b) and (e): control and FITC-labelled OLN-treated cells (green). Panels (c) and (f): merged images. Magnification: 63X.

FIGURE 4. Hypoxia and chitosan OLN effects on secretion of latent and active forms of gelatinases (MMP-2 and MMP-9) by human keratinocytes. HaCaT keratinocytes (10^6 cells/2 ml Panserin 601 medium) were left untreated or treated with 200 μl chitosan OLNs, chitosan OFNs, or OSS for 24 h in normoxia (20% O_2; panel a: lanes 1-4; panels b-d: black columns) or hypoxia (1% O_2; panel a: lanes 5-8; panels b-e: white columns). After collection of cell supernatants, MMP-2 and MMP-9 latent/active forms were analysed by gelatin zymography (panel a) and subsequent densitometry (panels b-d). Recombinant human MMP-9 (83 kDa) was employed as a standard marker (st). Results are shown as a representative gel (panel a) or means+SEM (panels b-d) from three independent experiments. Densitometric data were also evaluated for significance by ANOVA: * vs normoxic control cells: $p<0.005$ (panel b), $p<0.0001$ (panel c), and $p<0.0001$ (panel d); ° vs hypoxic control cells: $p<0.003$ (panel b), $p<0.0001$ (panel c), and $p<0.0001$ (panel d).

FIGURE 5. Hypoxia and chitosan OLN effects on protein levels of gelatinases (MMP-2 and MMP-9) secreted by human keratinocytes. HaCaT keratinocytes (10^6 cells/2 ml Panserin 601 medium) were left untreated or treated with 200 µl chitosan OLNs, chitosan OFNs, or OSS for 24 h in normoxia (20% O_2; black columns, both panels) or hypoxia (1% O_2; white columns, both panels). After collection of cell supernatants, MMP-2 (panel a) and MMP-9 (panel b) protein levels were quantified by ELISA. Results are shown as means+SEM from three independent experiments. Data were also evaluated for significance by ANOVA: * vs normoxic control cells: $p<0.0001$ (panel a) and $p<0.0001$ (panel b); ° vs hypoxic control cells: $p<0.0001$ (panel a) and $p<0.0001$ (panel b).

FIGURE 6. Hypoxia and chitosan OLN effects on protein levels of gelatinase inhibitors (TIMP-1 and TIMP-2) secreted by human keratinocytes. HaCaT keratinocytes (10^6 cells/2 ml Panserin 601 medium) were left untreated or treated with 200 µl chitosan OLNs, chitosan OFNs, or OSS for 24 h in normoxia (20% O_2; black columns, both panels) or hypoxia (1% O_2; white columns, both panels). After collection of cell supernatants, TIMP-1 (panel a) and TIMP-2 (panel b) protein levels were quantified by ELISA. Results are shown as means+SEM from three independent experiments. Data were also evaluated for significance by ANOVA: * vs normoxic control cells: p not significant (panel a) and $p<0.03$ (panel b); ° vs hypoxic control cells: p not significant (panel a) and $p<0.004$ (panel b).

FIGURE 7. Hypoxia and chitosan OLN effects on balances between gelatinases and their inhibitors secreted by human keratinocytes. MMP-9/TIMP-1 and MMP-

2/TIMP-2 stoichiometric ratios were calculated after results from ELISA investigation (see Figs 4-5). Results are shown as means+SEM from three independent experiments. Data were also evaluated for significance by Student's *t* test: * vs normoxic control cells: $p<0.05$ (panel a) and $p<0.001$ (panel b); ° vs hypoxic control cells: $p<0.02$ (panel a) and $p<0.02$ (panel b).

Table 1

OLN preparation	diameter nm ± SD	polydispersity index	zeta potential mV ± SD
preparation no.1	710.40 ± 116.3	0.23	+35.56±1.00
preparation no.2	766.70 ± 142.4	0.22	+35.84±1.00
preparation no.3	735.57± 123.4	0.23	+34.97±1.00

Table 2

OFN preparation	diameter nm ± SD	polydispersity index	zeta potential mV ± SD
preparation no.1	222.8 ± 103.4	0.12	+34.74 ± 1.00
preparation no.2	263.7 ± 175.3	0.12	+34.69 ± 1.00
preparation no.3	245.1 ± 146.7	0.12	+34.57 ± 1.00

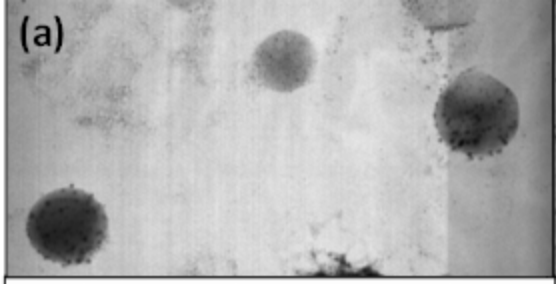
(a)

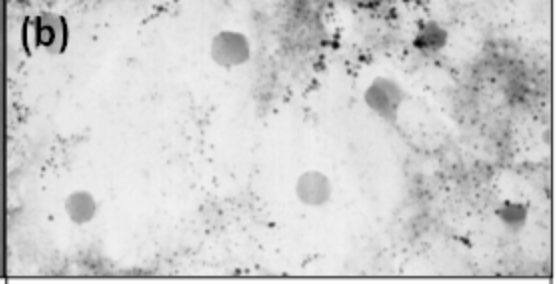
(b)

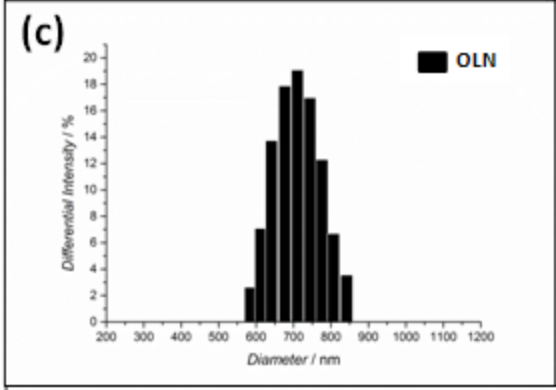
(c)
OLN
Differential Intensity / %
Diameter / nm

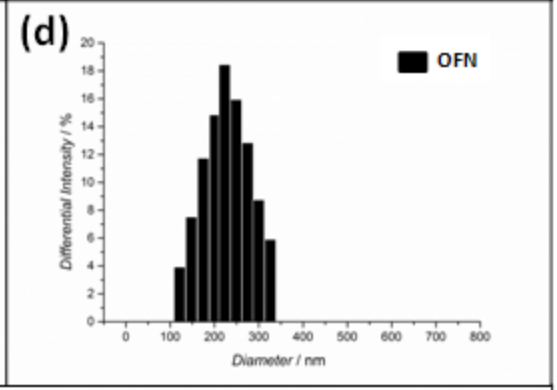
(d)
OFN
Differential Intensity / %
Diameter / nm

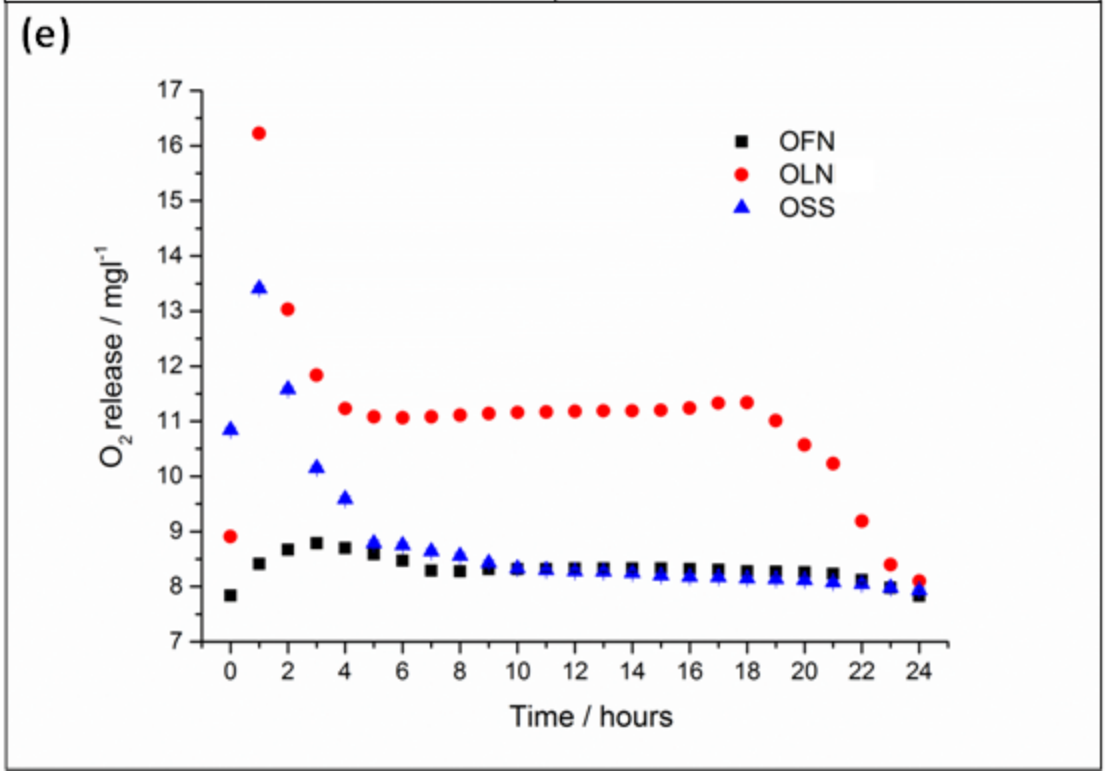
(e)
OFN
OLN
OSS
O2 release / mgl-1
Time / hours

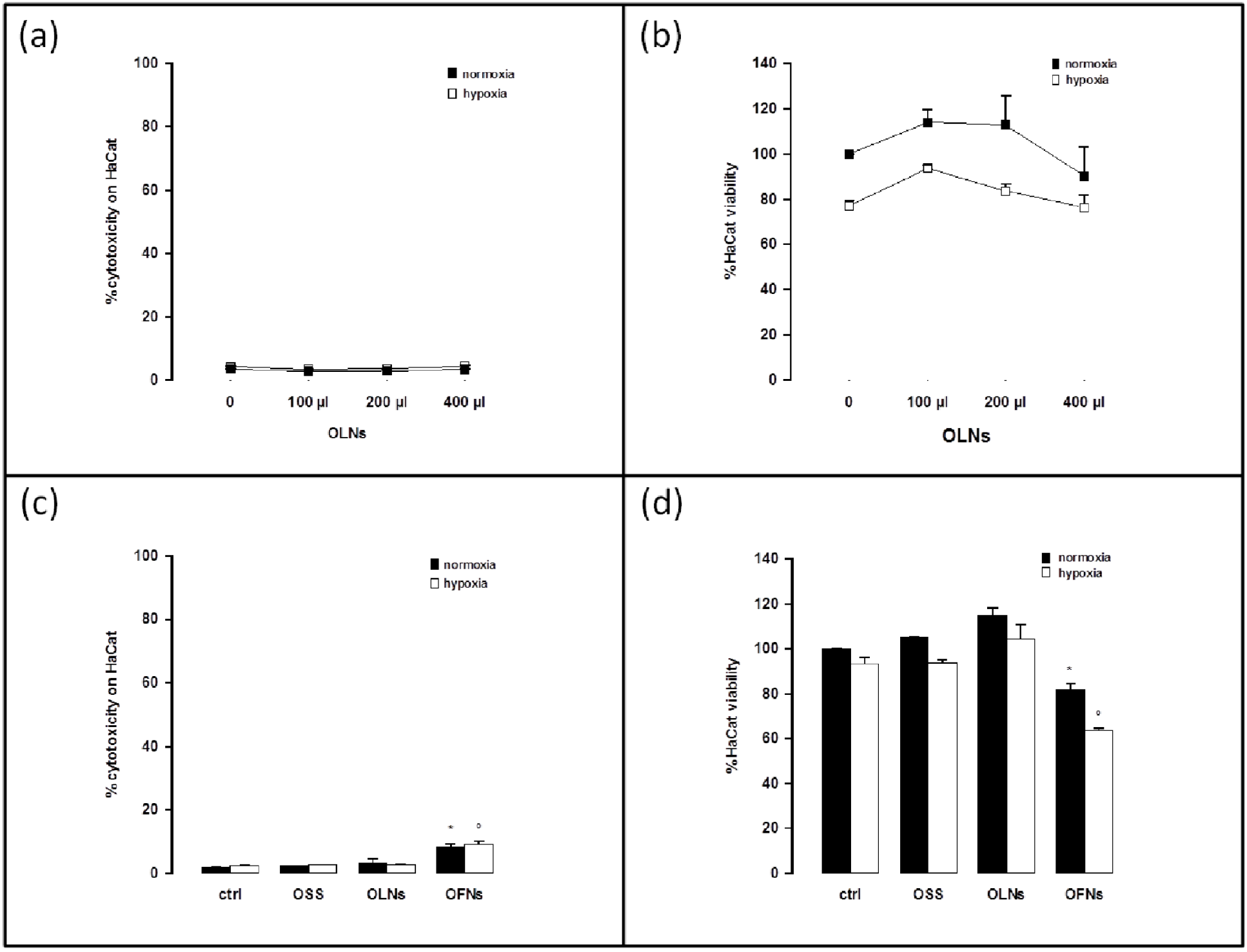
(a)
100
80
60
40
20
0
% cytotoxicity on HaCat
normoxia
hypoxia
0
100 µl
200 µl
400 µl
OLNs
(b)
140
120
100
80
60
40
20
0
% HaCat viability
normoxia
hypoxia
0
100 µl
200 µl
400 µl
OLNs
(c)
100
80
60
40
20
0
% cytotoxicity on HaCat
normoxia
hypoxia
*
°
ctrl
OSS
OLNs
OFNs
(d)
140
120
100
80
60
40
20
0
% HaCat viability
normoxia
hypoxia
*
°
ctrl
OSS
OLNs
OFNs

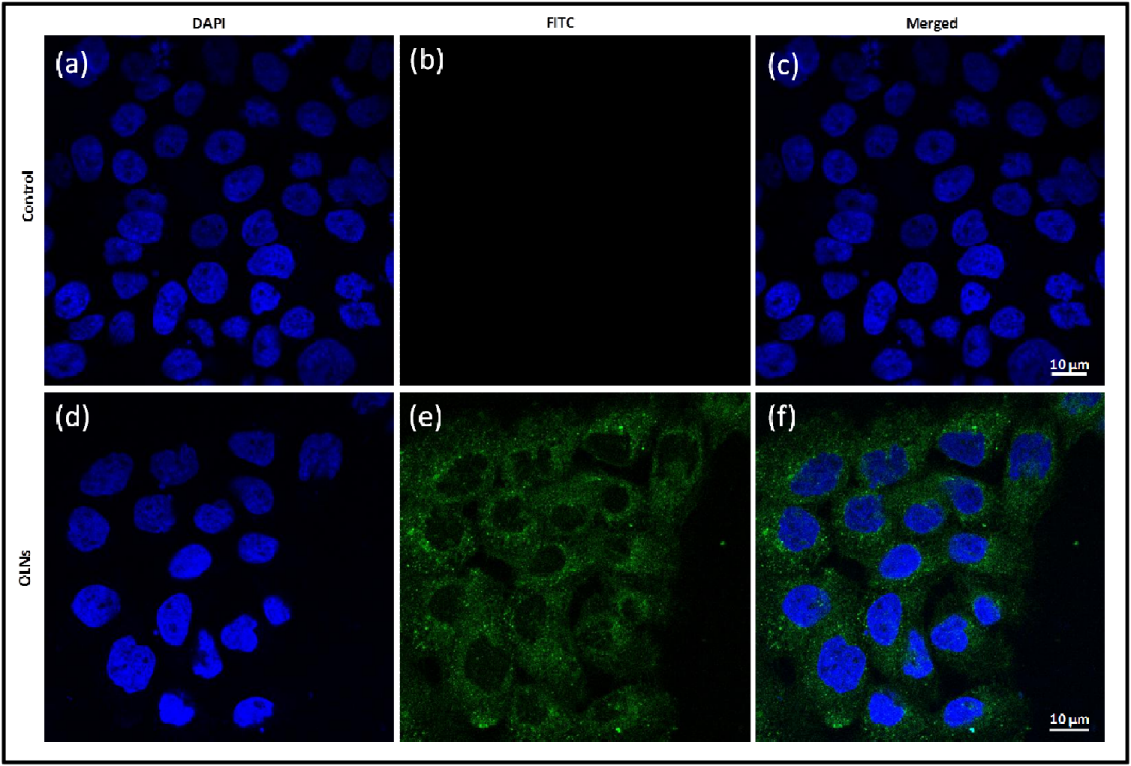
DAPI
FITC
Merged
Control
QUNs
(a)
(b)
(c)
(d)
(e)
(f)
10 µm
10 µm

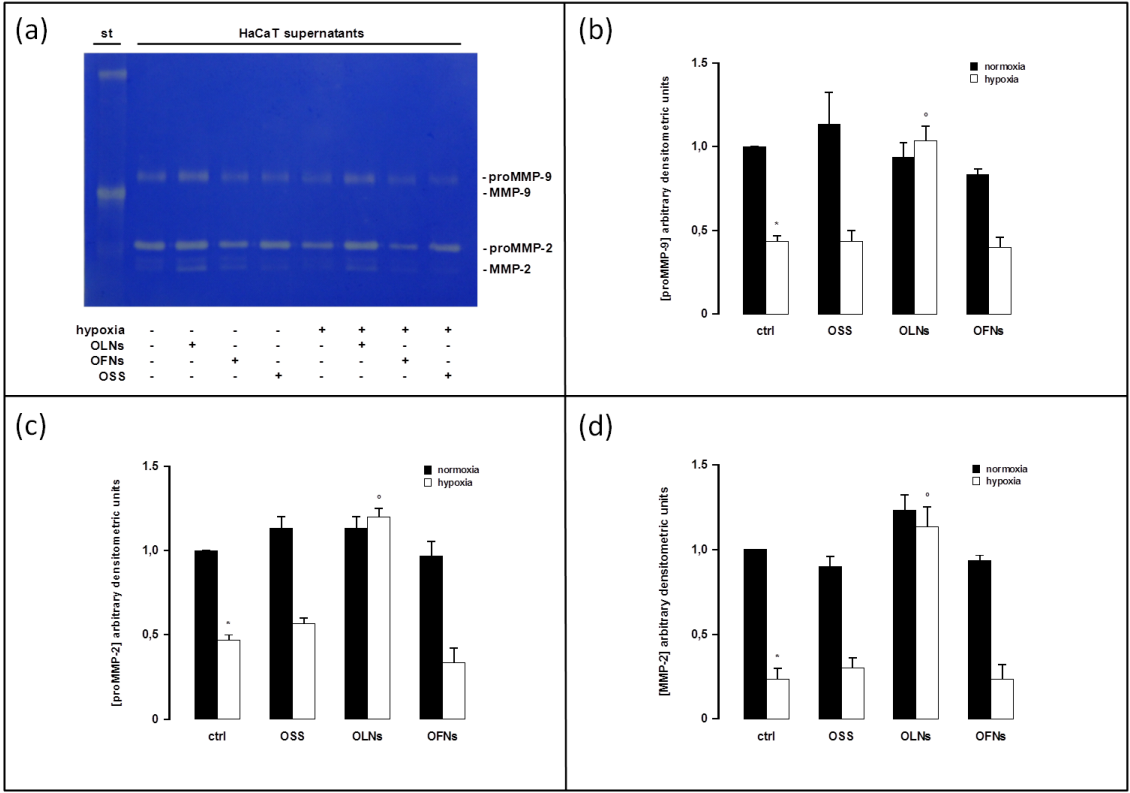
(a)
st
HaCaT supernatants
- proMMP-9
- MMP-9
- proMMP-2
- MMP-2
hypoxia - - - - + + + +
OLNs - + - - - + - -
OFNs - - + - - - + -
OSS - - - + - - - +
(b)
[proMMP-9] arbitrary densitometric units
normoxia
hypoxia
1.5
1,0
0,5
0
ctrl
OSS
OLNs
OFNs
(c)
[proMMP-2] arbitrary densitometric units
normoxia
hypoxia
1.5
1,0
0,5
0
ctrl
OSS
OLNs
OFNs
(d)
[MMP-2] arbitrary densitometric units
normoxia
hypoxia
1.5
1,0
0,5
0
ctrl
OSS
OLNs
OFNs

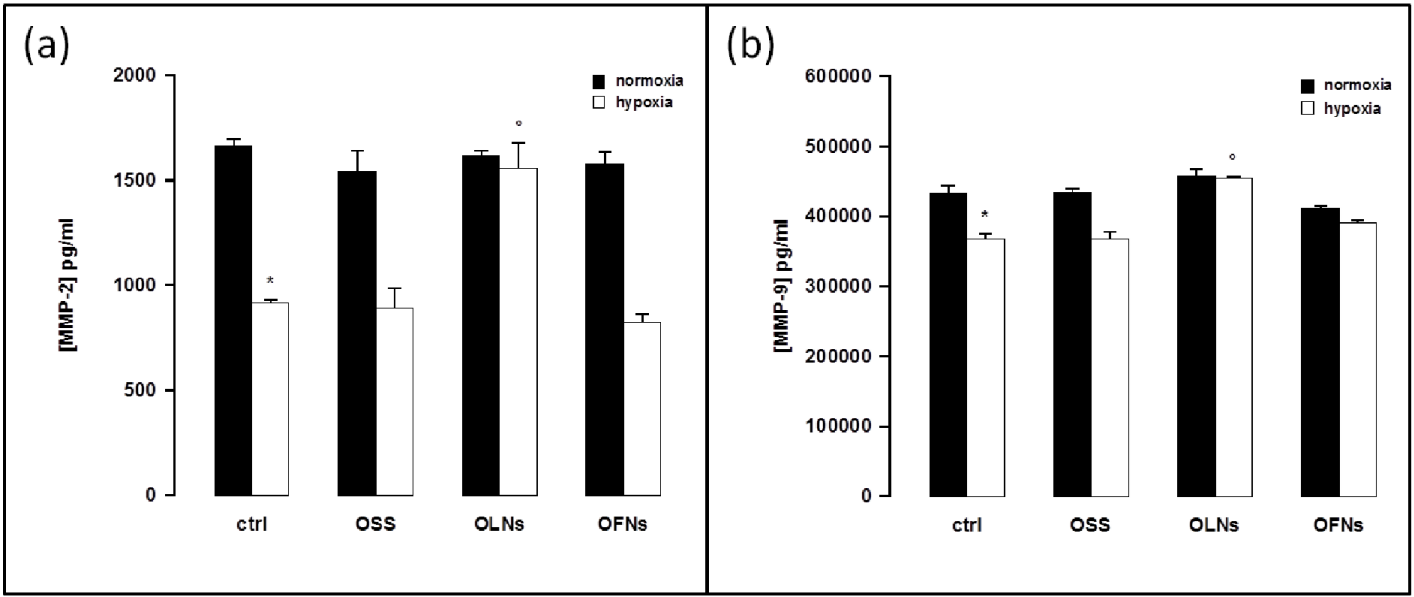
(a)
2000
1500
1000
500
0
[MMP-2] pg/ml
normoxia
hypoxia
*
°
ctrl
OSS
OLNs
OFNs
(b)
600000
500000
400000
300000
200000
100000
0
[MMP-9] pg/ml
normoxia
hypoxia
*
°
ctrl
OSS
OLNs
OFNs

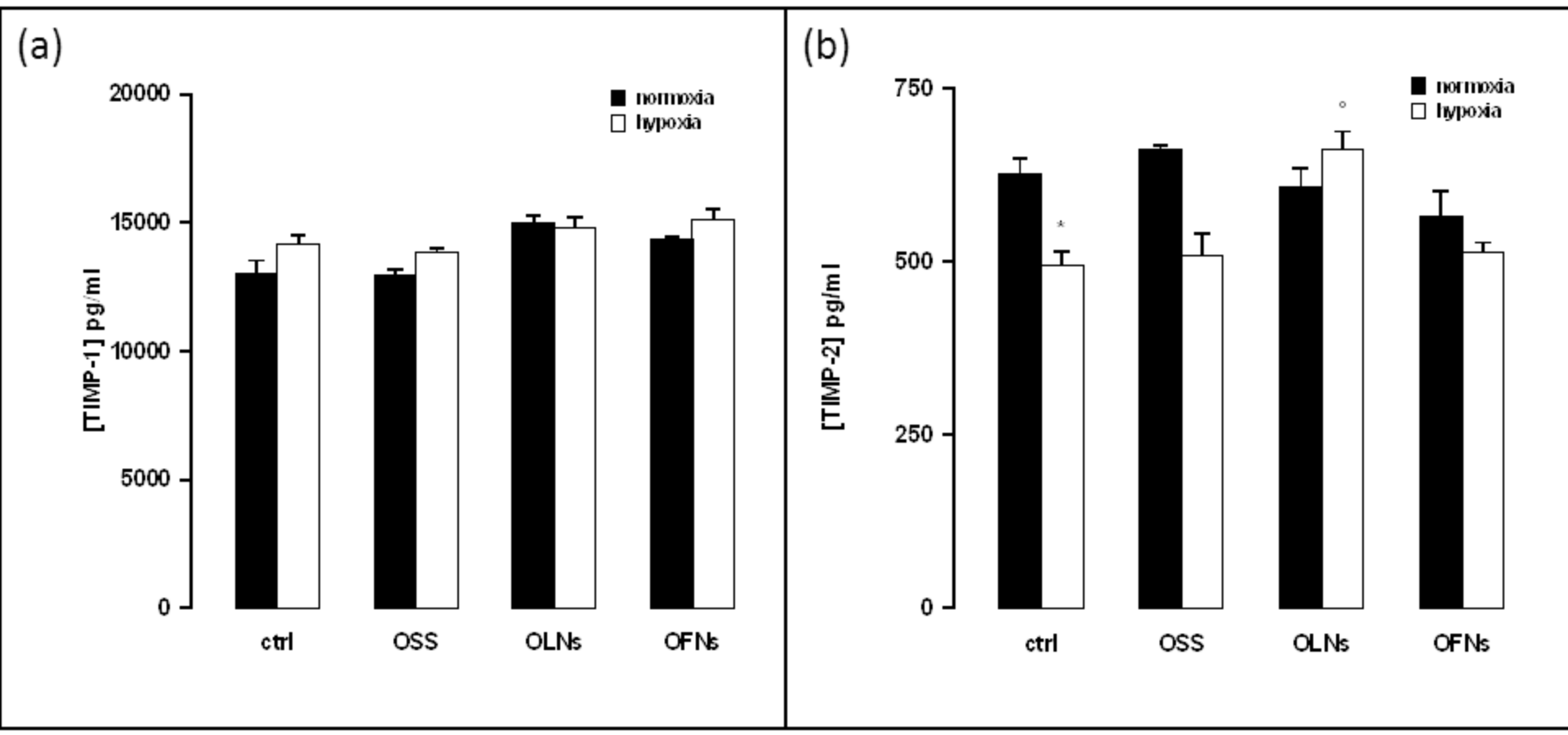
(a)
20000
15000
10000
5000
0
[TIMP-1] pg/ml
normoxia
hypoxia
ctrl
OSS
OLNs
OFNs
(b)
750
500
250
0
[TIMP-2] pg/ml
normoxia
hypoxia
*
°
ctrl
OSS
OLNs
OFNs

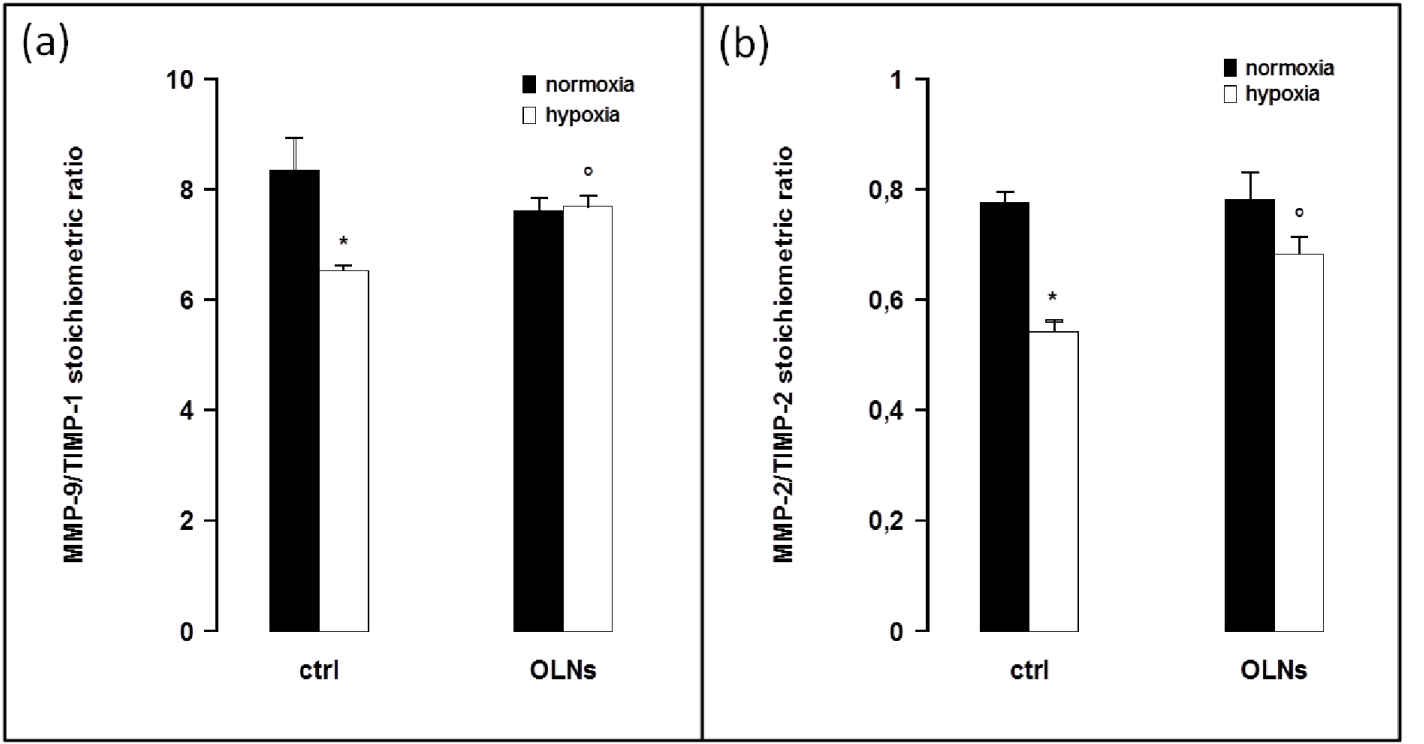
(a)
MMP-9/TIMP-1 stoichiometric ratio
10
8
6
4
2
0
normoxia
hypoxia
*
°
ctrl
OLNs
(b)
MMP-2/TIMP-2 stoichiometric ratio
1
0,8
0,6
0,4
0,2
0
normoxia
hypoxia
*
°
ctrl
OLNs